Ca^{2+} Coordination to Backbone Carbonyl Oxygen Atoms in Calmodulin and Other EF-Hand Proteins: ^{15}N Chemical Shifts as Probes for Monitoring Individual-Site Ca^{2+} Coordination†

Rodolfo R. Biekofsky,‡ Stephen R. Martin,§ J. Peter Browne,§ Peter M. Bayley,*,§ and James Feeney*,‡

Molecular Structure Division and Physical Biochemistry Division, National Institute for Medical Research, The Ridgeway, Mill Hill, London NW7 1AA, U.K.

Received January 7, 1998; Revised Manuscript Received March 17, 1998

ABSTRACT: Examination of the NMR ^{15}N chemical shifts of a number of EF-hand proteins shows that the shift value for the amido nitrogen of the residue in position 8 of a canonical EF-hand loop (or position 10 of a pseudo EF-hand loop) provides a good indication of metal occupation of that site. The NH of the residue in position 8 is covalently bonded to the carbonyl of residue 7, the only backbone carbonyl that coordinates to the metal ion in a canonical EF-hand loop. Upon metal coordination to this carbonyl, there is an appreciable deshielding of the ^{15}N nucleus at position 8 (+4 to +8 ppm) due to the polarization of the O(7)═C(7)−N(8) amido group and the corresponding reduction in the electron density of the nitrogen atom. This deshielding effect is effectively independent of the binding of metal to the other site of an EF-hand pair, allowing the ^{15}N shifts to be used as probes for site-specific occupancy of metal binding sites. In addition, a Ca^{2+}-induced change in side-chain H_α-C_α-C_β-H_β torsion angle for isoleucine or valine residues in position 8 can also contribute to the deshielding of the amide ^{15}N nucleus. This conformational effect occurs only in sites I or III and takes place upon binding a Ca^{2+} ion to the other site of an EF-hand pair (site II or IV) regardless of whether the first site is occupied. The magnitude of this effect is in the range +5 to +7 ppm. A Ca^{2+} titration of ^{15}N-labeled apo-calmodulin was performed using 2D ^1H-^{15}N HSQC NMR spectra. The changes in the ^{15}N chemical shifts and intensities for the peaks corresponding to the NH groups of residues in position 8 of the EF-hand loops allowed the amount of metal bound at sites II, III and IV to be monitored directly at partial degrees of saturation. The peak corresponding to site I could only be monitored at the beginning and end of the titration because of line broadening effects in the intermediate region of the titration. Sites III and IV both titrate preferentially and the results demonstrate clearly that sites in either domain fill effectively in parallel, consistent with a significant positive intradomain cooperativity of calcium binding.

EF-hand calcium binding proteins (CaBPs)[1] such as calmodulin (CaM) and troponin C (TnC) enable the cell to detect a stimulatory influx of Ca^{2+} and thereby to transduce this signal into a variety of cellular processes that often require a rapid response. The mechanism of this molecular switch involves a dynamic conformational change induced in the protein by Ca^{2+} binding (*1*−*4*). These proteins are characterized by highly conserved helix-loop-helix calcium-binding domains known as EF-hand motifs (*5*). Calmodulin, for example, has two structurally similar globular domains each containing a pair of EF-hands and can therefore bind a total of four Ca^{2+} ions.

Ca^{2+} binding to EF-hand proteins or to their isolated fragments has been extensively examined using biophysical techniques. Microcalorimetry can report thermodynamic changes associated with the metal binding to these proteins (*6*, *7*). Both fluorescence and CD methods monitor the global conformational changes accompanying metal ion binding (*8*−*14*). NMR can report information related to individual atoms throughout the sequence. Several ^1H studies have used chemical shift changes to monitor the effects of Ca^{2+} binding (*15*−*17*). Multidimensional NMR in combination with $^{13}C/^{15}N$ double labeling of the proteins has largely overcome signal overlap problems, thus, simplifying the NMR signal assignments.

The availability of ^{15}N labeled proteins facilitates the use of ^{15}N chemical shifts as probes for monitoring Ca^{2+} titrations. Recently, Li and co-workers reported the Ca^{2+} titration of the N-domain of troponin C (NTnC) using 2D ^1H-^{15}N HSQC NMR (*18*). They showed that several different types of Ca^{2+}-induced chemical shifts appear within the amino acid sequence, and these did not allow the direct

† This work was supported by funds from the Medical Research Council. R.R.B. was supported by a Marie Curie Fellowship from the Commission of the European Communities and a Travelling Research Fellowship from the Wellcome Trust.

* To whom correspondence should be addressed. E-mail: jfeeney@nimr.mrc.ac.uk and pbayley@nimr.mrc.ac.uk.

‡ Molecular Structure Division.

§ Physical Biochemistry Division.

[1] Abbreviations: NMR, nuclear magnetic resonance; HSQC, heteronuclear single quantum coherence; CD, circular dichroism; CaBPs, calcium-binding proteins; CaM, calmodulin; C-CaM; C-domain of calmodulin; sTnC, skeletal troponin C; cTnC, cardiac troponin C; N-TnC, N-domain of troponin C.

S0006-2960(98)00044-0 CCC: $15.00
Published on Web 04/30/1998

Table 1: Comparison of Ligand Positions and Ligand Groups in Canonical and Pseudo EF-Hand Binding Sites

Canonical EF-Hand												
position[a]	1	2	3	4	5	6	7	8	9	10	11	12
ligand coordinate[b]	**X**		**Y**		**Z**		**-Y**		**-X**			**-Z**
ligand group[c]	COO^-/ /$CONH_2$		COO^-/ /$CONH_2$		COO^-/ /$CONH_2$		C═O		H_2O			O═C−O^-
consensus sequence[d]	D	bas	D/N	G	D/N	G	*x*	hyd.	D/E/T/S	hyd.	ac.	E
example												
calmodulin[e] site I	D	K	D	G	D	G	**T**	I	T	T	K	E
calmodulin[e] site II	D	A	D	G	N	G	**T**	I	D	F	P	E
calmodulin[e] site III	D	K	D	G	N	G	**F**	I	S	A	A	E
calmodulin[e] site IV	N	I	D	G	D	G	**Q**	V	N	Y	E	E
$calbindin_{9k}$ site II	D	K	N	G	D	G	**E**	V	S	F	E	E
Pseudo EF-Hand												
position	1	2	3	4	5	6	7	8	9	10	11	12	13	14
ligand coordinate	**X**			**Y**		**Z**			**-Y**		**-X**			**-Z**
ligand group	C═O			C═O		C═O			C═O		COO^-/OH/ /$CONH_2$			O═C−O^-
example														
$calbindin_{9k}$ site I	**A**	A	K	**E**	G	**D**	P	N	**Q**	L	S	K	E	E

[a] The position number is based on the consensus sequence for a canonical EF-hand (*23*). [b] The coordinates of the Ca^{2+} are shown in bold, and the underlined coordinate has a backbone carbonyl oxygen as the Ca^{2+} ligand, based on previously determined structures of EF-hand proteins (*81*). Residues with backbone carbonyl oxygen atoms that coordinate Ca^{2+} are shown in bold and underlined. [c] The notation COO^- is used to indicate a carboxylate group that binds Ca^{2+} in a monodentate manner and O═C−O^- is used to indicate a carboxylate group that binds Ca^{2+} in a bidentate manner. [d] Abbreviations include: ac. for acidic residue, bas. for basic residue, hyd. for hydrophobic residue and *x* for any residue. [e] *Drosophila melanogaster* calmodulin.

assignment of the relative affinity of sites I and II of the N-domain. Ca^{2+} binding to the N-terminal domain of yeast calmodulin has also been monitored by examining 2D ^1H-^{15}N HSQC spectra of samples containing different Ca^{2+} concentrations (*19*). The observed spectral changes induced by Ca^{2+}-binding were difficult to classify and there was no apparent relationship between the spectral change and the amino acid type and location, suggesting that the local changes in conformation and dynamics accompanying Ca^{2+} binding appeared to differ from residue to residue. With the increasing use of ^1H-^{15}N HSQC spectra for monitoring calcium-binding events (*12*, *20*, *21*), a more detailed understanding of the different factors affecting the nitrogen chemical shifts is required in order to improve the structural analysis.

The consensus EF-hand motif spans 29 residues and consists of a loop flanked by two α-helices. A 12 residue segment, normally referred to as the EF-hand loop, although it comprises the loop and the end of the F helix, contains all of the calcium-binding ligands. The calcium ion is coordinated by seven oxygens in a pentagonal bipyramidal arrangement. The calcium ligands are labeled according to an octahedral arrangement, with one vertex -Z shared by the two carboxyl oxygen atoms of a glutamate side chain that binds in a bidentate mode to the Ca^{2+}, position -Y occupied by a conserved backbone carbonyl group and -X being generally a water molecule (see Table 1) (*22*−*25*).

The backbone carbonyl oxygen ligand is formally neutral and forms part of a polarizable π system with the adjacent nitrogen atom. While interactions of side-chain carboxylate or carboxamide oxygen atoms with the calcium ion would not be expected to have large inductive shielding effects on the backbone NH nuclei, interactions of the main-chain carbonyl group with the cation would offer the possibility of a direct shielding perturbation of the neighboring backbone NH nuclei. In a canonical EF-hand loop, the carbonyl in position 7 is the only backbone carbonyl that coordinates directly to calcium (Table 1): this might be expected to confer a unique shielding characteristic on the NH of the residue in position 8 in its response to the binding of calcium.

The present study focuses on the ^{15}N-shielding changes upon Ca^{2+} coordination of the O(7)═C(7)−N(8) amido group and examines the possibility of using the perturbation of this amido nitrogen atom as a probe of site-specific Ca^{2+} occupation. The available body of ^{15}N chemical shifts of a number of EF-hand proteins from the literature has been searched to find correlations between the shielding of the ^{15}N nucleus and different features of the electronic structure of proteins, in particular in their response to metal ion binding (*1*−*4*, *18*, *20*, *21*, *26*−*42*). A more detailed understanding of these effects should increase the value of ^{15}N chemical shifts as a means of obtaining structural information related to Ca^{2+} binding. As part of this study, a Ca^{2+} titration of ^{15}N-labeled apo-calmodulin using 2D ^1H-^{15}N HSQC NMR spectra has been carried out in order to evaluate the usefulness of these ^{15}N shieldings as probes for monitoring calcium binding.

EXPERIMENTAL PROCEDURES

Protein Expression and Purification. The cDNA coding for *Drosophila melanogaster* calmodulin, kindly supplied by K. Beckingham in the pOTSNco12 vector (*43*), was transformed into the *Escherichia coli* cell line AR58 (*26*) for expression of the ^{15}N labeled calmodulin. Four 1 L portions of bacterial cell culture were grown on minimal media ($K_2HPO_4 \cdot 3H_2O$ 14 g/L, KH_2PO_4 6 g/L, $MgSO_4 \cdot 7H_2O$ 0.2 g/L, sodium citrate$\cdot 7H_2O$ 1 g/L and D-glucose 10 g/L) supplemented with D-biotin 1 mg/L, thiamine-hydrochloride 10 μM, ampicillin 100 mg/mL, and $(^{15}NH_4)_2SO_4$ (ISOTECinc) 1 g/L, and were harvested after 4 h of heat shock treatment as described by Shatzman and Rosenberg (*44*). The calmodulin was isolated and purified to homogeneity as described elsewhere (*45*).

Sample Preparation. The purified calmodulin was concentrated to 2 mM in 25 mM Tris HCl, pH 7.5, 500 mM

KCl, and 5 mM EDTA. The apo protein was prepared by first treating with a further 10 mM EDTA and then passing through a Pharmacia PD10, Sephadex G25 column equilibrated and eluted with 111 mM KCl which had been pretreated with Chelex (Sigma). The pH of the eluted protein was adjusted to pH 6.5 and the sample brought to a final concentration of 1.368 mM in 90% H_2O:10% D_2O, calculated using $\epsilon_{259\ nm} = 2179 M^{-1}\ cm^{-1}$ (*43*).

NMR Spectra. ^1H-^{15}N heteronuclear single quantum coherence (HSQC) spectra (*46*, *47*) were recorded on a Varian 500 NMR spectrometer at 25 °C and acquired with ^{15}N decoupling during the acquisition period. Each spectrum was collected with 256 complex data points in the t_2 dimension and 1088 complex data points in the t_1 dimension; 16 transients per FID were recorded. The ^1H and ^{15}N sweep widths were 7199.4 and 2500 Hz, respectively. Suppression of the water resonance was achieved by the Watergate method (*48*). Total acquisition time for each spectrum was 3 h. Data were zero-filled in both dimensions to generate a final 512 × 2048 points spectrum. The data sets were processed using the Felix software package (Felix, version 2.3, 1993, Biosym Technologies, Inc., San Diego). Volumes were measured using routines within XEASY (*49*) at a low contour threshold using an elliptical integration mode. Chemical shifts of ^1H resonances were measured from an internal standard dioxane and referenced to 5,5-dimethyl-5-silapentane-2-sulfonate (taken as 3.750 ppm from dioxane) (*50*). ^{15}N chemical shifts are referenced to liquid NH_3 using the frequency ratio method ($^{15}N/^1H = 0.101\ 329\ 118$) (*50*).

Calcium Titration. 2D ^1H-^{15}N HSQC NMR spectra were recorded for calmodulin at various Ca^{2+} concentrations from 0 to 5 equiv of the concentration of the calmodulin. The signals in the spectra are well resolved and individual amide NH $^1H/^{15}N$ resonances can be followed during the Ca^{2+} titration. The signals in the spectra of both apo and Ca^{2+}-saturated calmodulin have been assigned previously (*26*, *4*).

A stock solution of 50 mM $CaCl_2$ in 90% H_2O/10% D_2O was prepared from a standard 1 M $CaCl_2$ solution. For each titration point, an aliquot of 4 μL of this stock $CaCl_2$ solution was added to the NMR tube containing the calmodulin solution and mixed thoroughly. The changes in pH caused by $CaCl_2$ additions were negligible.

RESULTS

^{15}N Chemical Shift Differences upon Ion Binding. (a) Canonical EF-Hands. In the four calcium-binding loops of calmodulin and other calcium-binding proteins, the highly conserved hydrophobic residue in position 8 (usually Ile or Val) is involved in the structural linking of two paired calcium-binding sites via a short antiparallel β-sheet, characteristic of all EF-hand pairs (*23*) (see Figure 1). In Table 2, the ^{15}N chemical shifts for the NHs of position 8 are compared for calcium-free and calcium-loaded forms of several typical EF-hand pairs. Data from proteins where only one form (either the apo or holo) has been examined are also included in Table 2. In all cases, the ^{15}N nucleus in the NH groups of position 8 residues in the holo form is deshielded with respect to the apo form (Table 2). However, the corresponding chemical shift difference differs in magnitude according to whether it is the first site (I or III) or the second site (II or IV) of the EF-hand pair. In the case

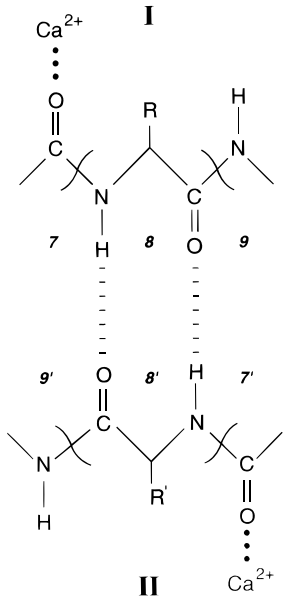

FIGURE 1: Schematic drawing of antiparallel β-sheet characteristic of canonical EF-hand pairs.

of sites I or III, the magnitude of this effect is in the range +14 to +16 ppm, and is considerably larger than for sites II or IV where the range is +4 to +8 ppm. The difference in magnitude of this effect between sites I or III and sites II or IV appears to be related to a difference in the shieldings in the apo form: in the calcium-loaded form the chemical shifts for the NHs of the residues in position 8 are around 124−127 ppm for all four sites, whereas in the apo form these shifts are in the ranges 111−114 ppm for site I or III and 118−120 ppm for site II or IV.

Calmodulin, in both the apo and holo states, can form complexes with target peptides, and such binding has been shown to cause global conformational changes in the proteins involving the relative positions of the domains (*51*, *52*). Table 3 shows that in all cases examined, the binding of the peptide to the protein has little or no effect on the loop position 8 ^{15}N chemical shifts. This insensitivity to peptide binding increases the specificity of the ^{15}N chemical shifts of these particular nitrogens as direct probes for monitoring metal coordination at main chain carbonyl coordinating sites.

(b) Pseudo EF-Hands. Members of the S-100 family of proteins (*38*, *53*) are characterized by a modified ion-binding loop consisting of 14 residues as compared with the 12 residues of a calmodulin-like EF-hand (*54*). These pseudo EF-hands have four residues that coordinate Ca^{2+} by their main-chain carbonyl oxygens in positions 1, 4, 6, and 9 of the 14 residue loop (Table 1). The carbonyls of these residues form peptide bonds with the NH groups of the residues in positions 2, 5, 7, and 10, respectively. In Table 4A, the ^{15}N chemical shifts for the NH groups forming peptide bonds with the coordinating main-chain carbonyls are compared for some members of the S-100 family of proteins in their holo and apo forms. Chemical shift data have also been compared for their $(Cd^{2+})_2$ and apo forms in Table 4B. In the S-100 family of proteins, a pseudo EF-hand in site I (or III) is normally paired with a canonical EF-hand in site II (or IV). The residue in position 10 of the pseudo EF-hand and the residue in position 8 of the canonical EF-hand form part of a short antiparallel β-sheet that links

Table 2: ^{15}N Chemical Shift Difference for the NH of Residue in Position 8 of EF-Hand Loops in Ca^{2+}-Loaded (holo) and Ca^{2+}-Free (apo) Forms of Different Calcium Binding Proteins

	site I or III					site II or IV				
protein	site	res(8)[a]	δ(holo)[b]	δ(apo)[c]	$\Delta\delta$(h−a)[d]	site	res(8)[a]	δ(holo)[b]	δ(apo)[c]	$\Delta\delta$(h−a)[d]
calmodulin[e,f]	I	I27	127.1	111.0	+16.1	II	I63	124.0	119.8	+4.2
calmodulin[e,f]	III	I100	127.3	113.9	+13.4	IV	V136	125.2	120.0	+5.2
N-troponin C[g]	I	I37	125.9	111.9	+14.0	II	I73	126.5	118.3	+8.2
troponin C[h]	I	I37	126.4			II	I73	126.9		
troponin C[h]	III	I113	127.4			IV	I149	127.4		
oncomodulin[i]	I	L58	126.4			II	I97	124.4		
recoverin[j]	I	I44		116.7		II	L81		119.6	
recoverin[j]	III	I117		117.0		IV	L167		121.2	
spectrin[k]	I	L29		116.3		II	V72		117.3	

[a] res(8): residue in position 8 type and number in the protein sequence. [b] δ(holo): ^{15}N chemical shift (ppm) for the NH in Ca^{2+}-loaded (holo) form. [c] δ(apo): ^{15}N chemical shift (ppm) for the NH in Ca^{2+}-free (apo) form. [d] $\Delta\delta$(h−a): ^{15}N chemical shift difference (ppm) of Ca^{2+}-loaded (holo) minus Ca^{2+}-free (apo) forms. [e] Data for holo-calmodulin taken from ref *26*. [f] Data for apo-calmodulin (Ikura, M., personal communication). [g] Data for holo- and apo-N-troponin C taken from ref *18*. [h] Data for troponin C taken from refs *34* and *35*. [i] Data for oncomodulin taken from ref *37*. [j] Data for recoverin taken from ref *31*. [k] Data for apo-spectrin taken from ref *3* and from Pastore, A., personal communication.

Table 3: ^{15}N Chemical Shift Differences for the NH Residue in Position 8 of EF-Hand Loops in Peptide-Bound and Peptide-Free States in Both Apo-Calmodulin and in $(Ca^{2+})_4$-Calmodulin

		site I or III				site II or IV			
protein	peptide	res(8)[a]	δ(b)[b]	δ(f)[b]	$\Delta\delta$(b−f)[c]	res(8)[a]	δ(b)[b]	δ(f)[b]	$\Delta\delta$(b−f)[c]
apo-CaM[d]	neurom.	I27	112.0	111.0	+1.0	I63	120.4	119.8	+0.6
apo-CaM[d]	neurom.	I100	114.8	113.9	+0.9	V136	121.0	120.0	+0.1
$(Ca^{2+})_4$-CaM[e,f]	sk-mlck	I27	126.6	127.1	−0.5	I63	123.7	124.0	−0.3
$(Ca^{2+})_4$-CaM[e,f]	sk-mlck	I100	127.3	127.3	+0.0	V136	125.4	125.2	+0.2
$(Ca^{2+})_4$-CaM[g]	PFK	I27	127.1	127.1	+0.0	I63	123.6	124.0	−0.4
$(Ca^{2+})_4$-CaM[g]	PFK	I100	127.1	127.3	−0.2	V136	125.5	125.2	+0.3

[a] res(8): residue in position 8 type and number in the protein sequence. [b] δ(b), δ(f): ^{15}N chemical shift (ppm) for the indicated NH in peptide-bound and peptide-free states, respectively. [c] $\Delta\delta$(b−f): peptide-bound minus peptide-free ^{15}N chemical shift difference (ppm) for the indicated NH states. [d] Data for chicken apo-calmodulin with calmodulin-binding domain of neuromodulin taken from ref *36*. [e] Data for Ca^{2+} loaded *Drosophila* calmodulin with calmodulin-binding domain of skeletal myosin light-chain kinase taken from ref *28*. [f] Data for Ca^{2+} loaded *Drosophila* calmodulin taken from ref *26*. [g] Data for Ca^{2+} loaded *Drosophila* calmodulin with calmodulin-binding domain of phosphofructokinase from Biekofsky et al., unpublished results.

the two calcium-binding sites, similar to the β-sheet structure found in a pair of canonical EF-hands (Figure 1). From the data in Table 4, parts A and B, it appears that in all loops of the S-100 family of proteins so far examined, the ^{15}N nuclei of the NH groups adjacent to the backbone carbonyls involved in metal coordination are deshielded in the metal-loaded form compared to their shielding in the metal-free form, consistent with the trend observed for canonical EF-hand proteins in Table 2. The magnitude of this deshielding effect for residues in site II loops of the S-100 family (canonical EF-hand loops) is in the range +4 to +8 ppm similar to that observed in Table 2 for site II or IV loops in canonical EF-hand proteins (in the range +4 to +8 ppm). The magnitude of this effect for the NH groups of residues in position 10 of site I loops of the S-100 family (pseudo EF-hand loops) examined is in the range +4 to + 5 ppm (Table 4, parts A and B), similar to the values observed for the NHs of residues in position 8 of site II loops. The magnitudes for the differences in chemical shifts for the NHs in positions 2, 5, and 7 of the pseudo EF-hand loops are smaller and vary according to the position of the residue. This could be due to the fact that not all four backbone carbonyl groups in a pseudo EF-hand can adopt the spatial requirement for an optimal interaction with the metal ion (*55*−*57*). The replacement of calcium by cadmium as the metal ion yields similar trends in the observed chemical shift differences (Table 4B).

(c) Half-Saturated EF-Hands. The changes in chemical shift analyzed so far result from the binding of metal ions to both paired sites of an EF-hand pair. Two examples have been reported of ^{15}N data for an EF-hand pair with a metal ion bound exclusively to one site: $(Cd^{2+})_1$:calbindin$_{9k}$ and $(Ca^{2+})_1$:N-domain of cardiac troponin C.

$(Cd^{2+})_1$:Calbindin$_{9k}$. Akke and co-workers have observed that Cd^{2+} ions bind sequentially to calbindin$_{9k}$ and have used NMR to examine an ^{15}N enriched sample of calbindin$_{9k}$, which had one Cd^{2+} ion bound to site II (canonical EF-hand) and no metal ion bound to site I (pseudo EF-hand) (*29*, *56*). In Table 4C, the ^{15}N chemical shifts for the NH groups forming peptide bonds with the metal-coordinating main-chain carbonyls are compared for calbindin$_{9k}$ in the $(Cd^{2+})_1$ and apo forms. The chemical shift differences for these NH groups are presented in Table 4 and clearly indicate the metal occupancy of the sites for the metal-free, metal half-loaded, and metal-loaded species with either calcium or cadmium ions.

(i) Val61, the residue in position 8 of site II, shifts from 118.22 to 126.29 ppm (a difference of +8.07 ppm) upon binding the first cadmium to site II, and essentially does not shift (from 126.29 to 126.53 ppm, a difference of only +0.24 ppm) upon binding the second cadmium ion to site I.

(ii) Leu23, the residue in position 10 of site I, practically does not shift (from 120.33 to 120.27 ppm, a difference of only −0.06 ppm) upon binding the first cadmium to site II,

Table 4: ^{15}N Chemical Shift Differences for the NHs Adjacent to Coordinating Backbone Carbonyls in S-100 Family of Proteins

(A) Ca^{2+}-Loaded (Ca2) and Apo Forms in Calbindin$_{9k}$ and S100β

	site I (pseudo EF-hand loop)					site II (canonical EF-hand loop)				
protein	pos[a]	res[a]	δ(Ca2)[b]	δ(apo)[c]	$\Delta\delta$(Ca2-apo)[d]	pos[a]	res[a]	δ(Ca2)[b]	δ(apo)[c]	$\Delta\delta$(Ca2-apo)[d]
S100β[e,f]	2	G19	110.17	107.28	+2.89					
	5	G22	n.d.	109.13						
	7	K24	n.d.	126.12						
	10	L27	125.63	120.24	+5.39	8	C68	124.56	120.08	+4.48
calbindin$_{9k}$[g]	2	A15	116.77	114.19	+2.58					
	5	G18	112.87	108.21	+4.66					
	7	P20	*	*	*					
	10	L23	125.38	120.33	+5.05	8	V61	126.25	118.22	+8.03

(B) Cd^{2+}-Loaded (Cd2) and Apo Forms in Calbindin$_{9k}$

	site I (pseudo EF-hand loop)					site II (canonical EF-hand loop)				
protein	pos[a]	res[a]	δ(Cd2)[b]	δ(apo)[c]	$\Delta\delta$(Cd2-apo)[d]	pos[a]	res[a]	δ(Cd2)[b]	δ(apo)[c]	$\Delta\delta$(Cd2-apo)[d]
calbindin$_{9k}$[h]	2	A15	118.20	114.19	+4.01					
	5	G18	109.36	108.21	+1.15					
	7	P20	*	*	*					
	10	L23	124.33	120.33	+4.00	8	V61	126.53	118.22	+8.31

(C) Cd^{2+} Half-Loaded (Cd1) and Apo Forms in Calbindin$_{9k}$

	site I (pseudo EF-hand loop)					site II (canonical EF-hand loop)				
protein	pos[a]	res[a]	δ(Cd1)[b]	δ(apo)[c]	$\Delta\delta$(Cd1-apo)[d]	pos[a]	res[a]	δ(Cd1)[b]	δ(apo)[c]	$\Delta\delta$(Cd1-apo)[d]
calbindin$_{9k}$[g]	2	A15	113.76	114.19	−0.43					
	5	G18	109.23	108.21	+1.02					
	7	P20	*	*	*					
	10	L23	120.27	120.33	−0.06	8	V61	126.29	118.22	+8.07

[a] Abbreviations include pos for position in the EF-hand loop, res for residue type and number in the protein. [b] δ(Ca2), δ(Cd2), δ(Cd1): ^{15}N chemical shift (ppm) for the NH in Ca^{2+}-loaded, Cd^{2+}-loaded, and Cd^{2+} half-loaded form, respectively. [c] δ(apo): ^{15}N chemical shift (ppm) for the NH in Ca^{2+}-free (apo) form. [d] $\Delta\delta$(Ca2-apo), $\Delta\delta$(Cd2-apo), $\Delta\delta$(Cd1-apo): ^{15}N chemical shift difference (ppm) of Ca^{2+}-loaded minus apo (Ca^{2+}-free) forms, Cd^{2+}-loaded minus apo forms, and Cd^{2+} half loaded minus apo forms, respectively. [e] Data for calcium-bound human S100β taken from ref *42*. [f] Data for rat apo-S100β taken from refs *41* and *38*. [g] Data for $(Ca^{2+})_2$, $(Cd^{2+})_1$ half-loaded, and apo-calbindin D_{9k} taken from ref *29*. [h] Data for $(Cd^{2+})_2$ calbindin D_{9k} taken from ref *30*.

but shifts to 124.33 ppm (a difference of +4.06 ppm) upon binding the second cadmium to site I.

Thus, the chemical shift differences for these nitrogens in calbindin$_{9k}$ are good indicators of site-specific metal binding whereas most of the other NH signals of calbindin$_{9k}$ do not provide such information (*29*, *30*).

$(Ca^{2+})_1$:N-cTnC. Cardiac troponin C is an example of a canonical EF-hand protein with a pair of EF-hands in the N-domain that only binds one metal ion. Compared to skeletal troponin C, the mutation of critical side-chain ligands (D29L and D31A, positions 1 and 3 of site I) and an insertion (Val28) abolish the ability of site I to coordinate Ca^{2+} and only site II binds Ca^{2+} (*40*). The ^{15}N chemical shifts for the NH groups in position 8 residues taken from the $^1H/^{15}N$ HSQC spectra shown by Li and co-workers for the N-domain of this protein in the apo and half-saturated states (*21*) were analyzed.

(i) Residue Val72, position 8 of site II, shifts from ca. 115.4 to ca. 127.2 ppm (a difference of ca. +11.8 ppm) upon binding Ca^{2+} to site II and with no Ca^{2+} binding to site I; this shift difference is similar to that seen for holo N-sTnC [118.3 to 126.5 ppm for Ile73 of N-sTnC (Table 2)], where both paired sites are binding Ca^{2+}. Thus, the residue in position 8 of site II for both these proteins shifts in a similar manner upon binding Ca^{2+} to its site regardless of whether there is calcium ion binding to site I.

(ii) Residue Ile36, position 8 of site I, shifts from ca. 113.7 ppm to ca. 119.2 ppm (difference of ca. +5.5 ppm) upon binding Ca^{2+} to site II and no Ca^{2+} binding to site I; the residue in the analogous position in N-sTnC, Ile37, shifts from 111.9 to 125.9 ppm (a difference of +14.0 ppm) upon binding Ca^{2+} to both sites. The +8.5 ppm difference between +14.0 and +5.5 ppm is probably the effect of binding Ca^{2+} to its own site, whereas the ca. +5.5 ppm is due to an effect depending on the binding of Ca^{2+} to the other site of the EF-hand pair; such contributions can arise from changes in side-chain conformation induced by Ca^{2+} binding to the other site (see below).

^1H Chemical Shift Differences upon Ion Binding. The ^1H chemical shift differences observed on metal ion binding for position 8 (or 10 in pseudo EF-hands) NH groups vary from +1.5 to −0.3 ppm in the proteins examined (data not shown) and show no simple correlation with the occupancy of the sites. The ^1H chemical shift differences are much smaller than the ^{15}N shifts and are clearly more susceptible to anisotropic shielding contributions and to differences in shielding resulting from any changes in the strengths of hydrogen-bond interactions involving these NH groups.

Changes in Side-Chain Conformation upon Metal Binding. The residue in position 8 of canonical calcium binding EF-hands is a highly conserved isoleucine or valine (*24*). The H_α-C_α-C_β-H_β torsion angles for the isoleucine and valine residues in position 8 of canonical EF-hand loops were measured from the reported NMR and X-ray apo and holo structures (*1*, *2*, *4*, *28*, *32*−*35*, *58*−*68*). The values for this angle are presented in Tables 5 and 6, respectively. In the case of a family of NMR structures, the torsion angle was measured in each of the individual structures and the mean

Table 5: H_α-C_α-C_β-H_β Torsion Angle for Isoluecine or Valine Residues in Position 8 of Canonical EF-Hand Loops in NMR Solution Structures

(A) Metal-Free (apo) EF-Hand Pairs

			site I or III					site II or IV				
				H_α-C_α-C_β-H_β dihed[d]					H_α-C_α-C_β-H_β dihed[d]			
protein	PDB code[a]	n[b]	res(8)[c]	g(+)	trans	g(−)	σ_n[b]	res(8)[c]	g(+)	trans	g(−)	σ_n[b]
calmodulin	1CFC[e]	25	I27			−60.25	0.6	I63		−158.48		1.0
			I100			−65.15	6.9	V136		−154.28		1.8
calmodulin[f]	1DMO[f]	30	I27			−52.70	4.4	I63		−173.88		6.5
			I100			−61.58	5.1	V136		−175.00		9.1
Tr2C-CaM	1CMF[g]	20	I100			−104.33	17.7	V136	118.3			94.0
N-TnC	1TRF[h]	1	I37			−64.93	0.0	I73	64.77			0.0
calbindin	1CLB[i]	33	*	*	*	*	*	V61		171.30		10.5

(B) Metal-Loaded EF-Hand Pairs

			site I or III					site II or IV				
				H_α-C_α-C_β-H_β dihed[d]					H_α-C_α-C_β-H_β dihed[d]			
protein	PDB code[a]	n[b]	res(8)[c]	g(+)	trans	g(−)	σ_n[b]	res(8)[c]	g(+)	trans	g(−)	σ_n[b]
Tr2C-CaM	1CMG[j]	20	I100		171.95		2.9	V136		173.97		3.3
calmodulin	2BBN[k]	21	I27		161.73		12.2	I63		−135.46		51.4
			I100		−174.16		24.5	V136		−178.95		14.4
troponin C	1TNW[l]	23	I37		164.70		6.0	I73		154.89		2.3
			I113		170.13		4.5	I149		178.51		3.2
parvalbumin	2PAS[m]	9	I58		−163.17		9.1	I97		−179.30		5.3
calbindin	1CB1[n]	13	*	*	*	*	*	V61		−177.20		7.3

(C) Metal Half-Loaded EF-Hand Pairs

			site I or III					site II or IV				
				H_α-C_α-C_β-H_β dihed[d]					H_α-C_α-C_β-H_β dihed[d]			
protein	PDB code[a]	n[c]	res(8)[c]	g(+)	trans	g(−)	σ_n[b]	res(8)[c]	g(+)	trans	g(−)	σ_n[b]
calbindin	1CDN[o]	24	*	*	*	*	*	V61		172.13		8.0

[a] Protein Data Bank code (*95*). [b] *n*, number of NMR solution structures; σ_n, average standard deviation for the average H_α-C_α-C_β-H_β dihedral angle for the *n* number of NMR solution structures. [c] res(8): residue in position 8 type and number in the protein sequence. [d] H_α-C_α-C_β-H_β dihed: the H_α-C_α-C_β-H_β dihedral angle was measured in each of the *n* NMR solution structures, and the average angle is reported. [e] 1CFC: *Xenopus laevis* apo-calmodulin (*2*). [f] 1DMO: *X. laevis* apo-calmodulin (*4*). [g] 1CMF: apo C-terminal domain of *Bos taurus* calmodulin (*1*). [h] 1TRF: apo TR1C fragment of *Meleagris gallopavo* skeletal muscle troponin C (*32*). [i] 1CLB: bovine apo calbindin D9k (*67*). [j] 1CMG: Calcium-loaded C-terminal domain of *Bos taurus* calmodulin (*1*). [k] 2BBN: Calcium-bound *Drosophila melanogaster* calmodulin complexed with rabbit skeletal myosin light-chain kinase (calmodulin-binding domain) (*28*). [l] 1TNW: Calcium-loaded chicken skeletal muscle troponin C (*34*). [m] 2PAS: Calcium-loaded pike (*Esox lucius*) muscle parvalbumin (*33*). [n] 1CB1: Calcium-loaded porcine calbindin D9k (*65*). [o] 1CDN: $(Cd^{2+})_1$ bovine calbindin D9k (*64*).

value is reported.

For sites II or IV, the H_α-C_α-C_β-H_β torsion angle of the isoleucine (or valine) residue in position 8 appears not to change between the structures of the apo and holo forms. The side-chain conformation for this residue in both forms is trans; that is, the C_β-H_β and C_α-H_α bonds are at 180° to each other, so that H_β is pointing toward the other β-strand as shown in Figure 2A.

In contrast, for sites I or III, the side chain H_α-C_α-C_β-H_β torsion angle of the isoleucine residue in position 8 changes from gauche(−) in the structures for the apo form to trans in the structures for the holo form. In the apo form, the C_β-H_β and C_α-H_α bonds are at 60° to each other so that the ethyl moiety is pointing toward the other β-strand. In the holo form, C_β-H_β is rotated 180° from C_α-H_α, so that H_β is facing the opposite β-strand. Figure 2A shows the change in side-chain conformation for this residue upon Ca^{2+} binding to both sites of an EF-hand pair.

Peptide binding involves the interaction of peptide hydrophobic groups with the hydrophobic core of either domain, in which the loop residues at position 8 (Ile or Val) are essential components (*45*). It is interesting to notice that the side-chain conformation of the residues in position 8 in calcium-loaded peptide-bound calmodulin (2BBN in Table 5B) is similar to that in the calcium-loaded peptide-free (1CMG).

Ca^{2+} Binding Curves from the ^1H-^{15}N HSQC Spectra Titration. On the basis of the above analysis of the sensitivity of ^{15}N chemical shifts of specific resonances to metal binding to EF-hand loops, a Ca^{2+}-titration using 2D ^1H-^{15}N HSQC NMR spectra of ^{15}N-labeled *Drosophila melanogaster* calmodulin has been carried out. The previously assigned ^1H and ^{15}N resonances of both the apo and holo calmodulin were used to identify signals from nuclei showing spectral changes in their 2D ^1H-^{15}N HSQC NMR spectra accompanying the Ca^{2+} titration (*4*, *26*; Ikura, M., personal communication). Particular attention was focused on the residues in position 8 of the EF-hand loops of calmodulin. These residues are Ile27 and Ile63 for sites I and II in the N-domain and Ile100 and Val136 for sites III and IV in the C-domain.

For Ile100 and Val136 (sites III and IV), the changes throughout the Ca^{2+} titration occur in slow exchange and the data analysis involved measuring the volume of each peak of interest at each point in the titration. Figure 3B shows the peaks corresponding to the apo and holo forms for

Table 6: H_α-C_α-C_β-H_β Torsion Angle for the Residues in Position 8 of Canonical EF-Hand Loops in X-ray Structures of Calcium-Free (A) and Calcium-Loaded (B) Forms

(A) Metal-Free (apo) EF-Hand Pairs

		site I or III				site II or IV			
			H_α-C_α-C_β-H_β dihed[c]				H_α-C_α-C_β-H_β dihed[c]		
protein	PDB code[a]	res(8)[c]	g(+)	trans	g(−)	res(8)[c]	g(+)	trans	g(−)
troponin C	1NCZ[d]	I37			−61.95	I73	59.98		
troponin C	1TOP[e]	I37			−64.25	I73	50.50		
troponin C	1NCX[f]	I37			−58.48	I73	59.98		

(B) Metal-Loaded EF-Hand Pairs

		site I or III				site II or IV			
			H_α-C_α-C_β-H_β dihed[c]				H_α-C_α-C_β-H_β dihed[c]		
protein	PDB code[a]	res(8)[c]	g(+)	trans	g(−)	res(8)[c]	g(+)	trans	g(−)
calmodulin	1OSA[g]	I27		177.75		I63		−179.20	
		I100		179.07		V136		−176.43	
troponin C	1NCZ[d]	I113		−175.50		I149		175.03	
troponin C	1TOP[e]	I113		−175.99		I149		177.61	
troponin C	1NCX[g]	I113		171.73		I149		175.62	
parvalbumin	5CPV[h]	I58		175.32		I97		169.78	
parvalbumin	4CPV[i]	I58		173.44		I97		174.06	
parvalbumin	5PAL[j]	I58		175.54		I97		178.27	
parvalbumin	4PAL[k]	I58		179.48		I97		174.17	
calbindin	4ICB[l]	*	*	*	*	V61		162.14	

[a] Protein Data Bank code (*95*). [b] res(8): residue in position 8 type and number in the protein sequence. [c] H_α-C_α-C_β-H_β dihed: H_α-C_α-C_β-H_β dihedral angle. [d] 1NCZ: chicken $(Tb^{2+})_2$ skeletal muscle troponin C (*68*). [e] 1TOP: chicken $(Ca^{2+})_2$ skeletal muscle troponin C (*65*). [f] 1NCX: chicken $(Cd^{2+})_2$ skeletal muscle troponin C (*68*). [g] 1OSA: *Paramecium tetraurelia* $(Ca^{2+})_4$ calmodulin (*66*). [h] 5CPV: carp $(Ca^{2+})_2$ parvalbumin B (*58*). [i] 4CPV: carp $(Ca^{2+})_2$ parvalbumin (*59*). [j] 5PAL: leopard shark $(Ca^{2+})_2$ parvalbumin A (*62*). [k] 4PAL: Pike $(Ca^{2+})_1(Mg^{2+})_1$ parvalbumin (*60*). [l] 4ICB: bovine $(Ca^{2+})_2$ calbindin D9k (*61*)

residues Ile100 and Val136 in the HSQC spectrum after addition of 0.2725 equivalents of Ca^{2+}.

In contrast, the NMR spectral changes for Ile27 and Ile63 (sites I and II) occur in moderately fast exchange on the NMR chemical shift time scale leading to signals with averaged chemical shifts for the nuclei exchanging between bound and unbound species. Figure 4B shows the superposition of a portion of the ^1H-^{15}N HSQC spectra taken at different calcium additions showing the progressive shift of the peak corresponding to Ile63 (position 8 of site II) during the titration. The peak for Ile27, however, cannot be followed throughout the whole titration owing to extreme line broadening caused by the exchange during the intermediate part of the titration. The line width of the averaged signal under conditions of moderately fast exchange includes an additional exchange contribution that is proportional to the square of the chemical shift difference between the free and bound states and also varies with the fraction of bound species (*69*). These line-broadening effects will be noticed most readily in the intermediate parts of the titration for signals which have a very large shift difference between bound and free forms such as that of Ile27 where the shift difference is 16 ppm.

The volumes of the signals from residues in position 8 of EF-hand loops in sites III and IV of calcium-bound calmodulin were measured, and the changes in volume were normalized and plotted as a function of the $[Ca^{2+}]_{total}/[CaM]_{total}$ ratio (see Figure 5). The curves corresponding to signals from sites III and IV increase rapidly and in a parallel fashion during the addition of the first and second equivalent of Ca^{2+} and, at 2 equiv, show a site-occupation of about 70%. During the addition of the third and fourth Ca^{2+} equivalents they increase slowly to reach 100% occupation.

The resonances of residues in position 8 of EF-hand loops in sites I and II that show ^{15}N-chemical shift changes in the fast exchange limit during Ca^{2+} titration have been monitored, normalized according to $(\delta_{obs} - \delta_o)/(\delta_{final} - \delta_o)$, and plotted as a function of the $[Ca^{2+}]_{total}/[CaM]_{total}$ ratio (δ_{obs}, δ_o, and δ_{final} are the observed, apo and holo values of the chemical shift, respectively). The peak corresponding to Ile27 "disappears" after the initial additions in the titration and "reappears" later, and hence, the curve for site I is interrupted between 1 and 3.5 equiv. From the points available on the curve corresponding to site I, it would appear that the curves for sites I and II evolve in a parallel fashion, similar to the behavior observed for sites III and IV. The gradients of the curves corresponding to sites I and II increase slowly during addition of the first 2 equiv of Ca^{2+}, and increase rapidly in the region between 2 and 4 equiv.

The curves indicate that all four sites have some degree of occupation from the first addition of Ca^{2+} and that the occupation of all four sites is essentially completed when 4 equiv of Ca^{2+} have been added. The curves are consistent with the C-domain having higher calcium-binding affinity than the N-domain. The behavior for both domains indicates parallel filling of the calcium binding sites within each domain, which is fully consistent with a model of cooperativity between sites in the same domain.

The stoichiometric (or macroscopic) association constants for calcium binding to intact calmodulin and to its isolated N- and C-terminal domains are reasonably well established, at least at pH values in the range 7.5−8.0 (*70*−*72*). These constants allow one to calculate the concentrations of the various stoichiometric species present under particular concentration conditions but do not permit the calculation of the extent of occupancy of particular sites. Such calcula-

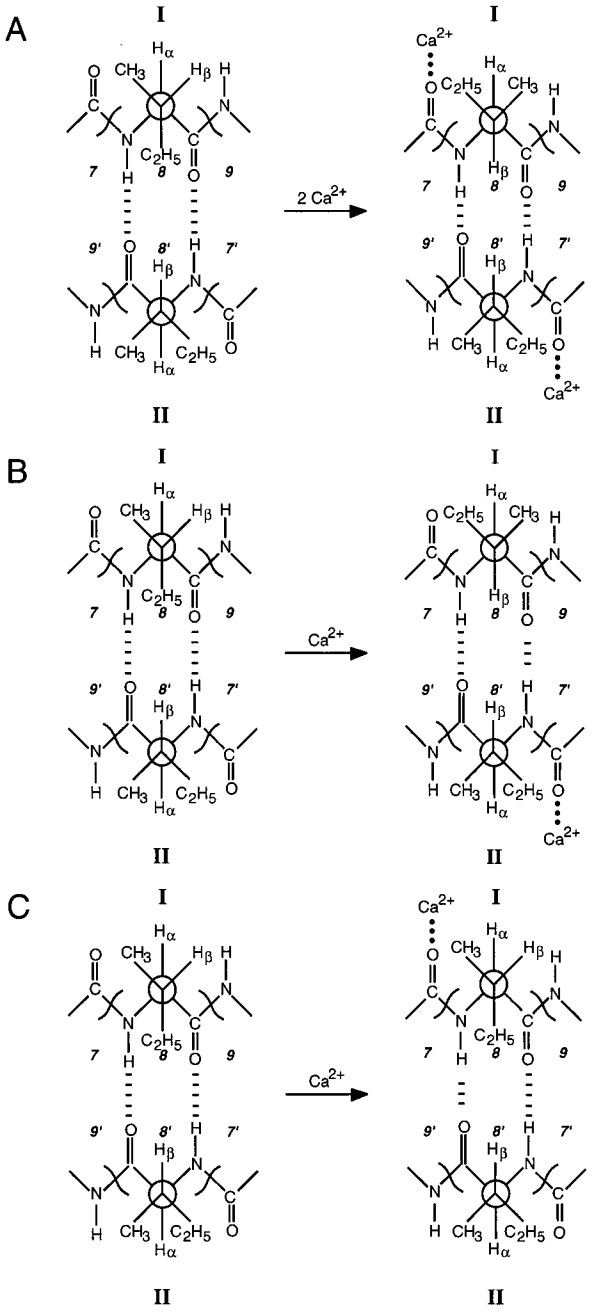

FIGURE 2: (A) Changes in side-chain conformation of β-sheet residues upon Ca^{2+} binding to both sites of an EF-hand pair (note change in site I). (B) Changes in side-chain conformation of β-sheet residues upon Ca^{2+} binding to only site II of an EF-hand pair (note change in site I). (C) Changes in side-chain conformation of β-sheet residues upon Ca^{2+} binding to only site I of an EF-hand pair (note no change in site I or II).

tions are only possible if the intrinsic (microscopic or site) association constants and the interaction (cooperativity) factors are known. These values cannot be calculated from the measured stoichiometric association constants for intact calmodulin but may be estimated from the corresponding constants for the isolated domains.

For the isolated N-terminal domain, the two measured stoichiometric constants, $K_1(N)$ and $K_2(N)$, are given by $K_1(N) = K_I + K_{II}$ and $K_2(N) = K_I K_{II} \alpha_N / K_1(N)$, where K_I and K_{II} are the site intrinsic binding constants and α_N is the factor by which the intrinsic affinity of one site within the domain is changed by occupancy of the other site. For the C-terminal domain, the corresponding expressions are $K_1(C) = K_{III} + K_{IV}$ and $K_2(C) = K_{III} K_{IV} \alpha_C / K_1(C)$. In the simplest case where the two sites within a domain have the same intrinsic affinity, then $K_I = K_{II} = K_1(N)/2$, $K_{III} = K_{IV} = K_1(C)/2$, $\alpha_N = 4K_2(N)/K_1(N)$, and $\alpha_C = 4K_2(C)/K_1(C)$. The values of these parameters may then be used to calculate the variation in individual site occupancy as a function of total added calcium. On the basis of inspection of the available published data (*25*, *72* and references therein), we assign a value for K_I ($=K_{II}$) in the range $(1-2) \times 10^4$ M^{-1} (with $\alpha_N = 15-60$) and K_{III} ($= K_{IV}$) in the range $(5-10) \times 10^4$ M^{-1} (with $\alpha_C = 30-100$). Using these ranges, we calculate that under the conditions of the NMR titration, the addition of 2 equiv of calcium would saturate 15−35% of the N-domain sites and 85−55% of the C-domain sites. The NMR data of Figure 5 are clearly consistent with this calculation.

The high degree of cooperativity (high α_C and α_N) means that a pair of sites within a domain must be filled effectively in parallel under these concentration conditions. It can be seen that the greater the divergence between the intrinsic affinities of a pair of sites (e.g., K_I, K_{II}), the greater will be the (apparent) cooperativity (e.g., α_N). The values of α_N and α_C derived on the assumption that $K_I = K_{II}$ and $K_{III} = K_{IV}$ therefore represent minimum estimates of the cooperativity. The values used in the calculations were derived from data obtained in the pH range 7.5−8, whereas the NMR data were obtained at pH 6.5. However, Milos and coworkers (*73*) have shown that although lowering the pH to 5.8 reduces the affinity of calmodulin for calcium, the effect is similar for both N- and C-domain sites, hence the deductions concerning cooperativity are not affected by the pH difference.

DISCUSSION

Origin of the ^{15}N Chemical Shift Changes upon Ca^{2+} Binding. ^{15}N shieldings are very sensitive to different intra- and intermolecular interactions (*74*, *75*). From the analysis of the data presented in this work, the origin of the observed ^{15}N deshielding of the residue in position 8 of canonical EF-hands (or 10 in pseudo EF-hands) resulting from calcium binding can be rationalized in terms of two main contributions:

(1) Changes in π-Polarization of the Peptide Bond. The C−N peptide bond has π-electron character due to the π-conjugation of the nitrogen lone pair. The coordination of a metal ion to the carbonyl oxygen of an amide group stabilizes the polarized resonance structure of the amide (resonance structure II) increasing the π-electron density of the oxygen and decreasing the π electron density of the nitrogen.

$$\underset{\text{I}}{[O{=}C{-}\ddot{N}} \leftrightarrow \underset{\text{II}}{{}^{-}O{-}C{=}N^{+}}] \xrightarrow{Ca^{2+}} [Ca^{2+}\cdots \underset{\text{I}}{O{=}C{-}\ddot{N}} \leftrightarrow Ca^{2+}\cdots \underset{\text{II}}{{}^{-}O{-}C{=}N^{+}}]$$

For an amide group, the enhancement of the delocalization of the nitrogen lone-pair upon metal coordination to the carbonyl oxygen is expected to yield a deshielding effect to the NMR of the ^{15}N nucleus. There have been few reports

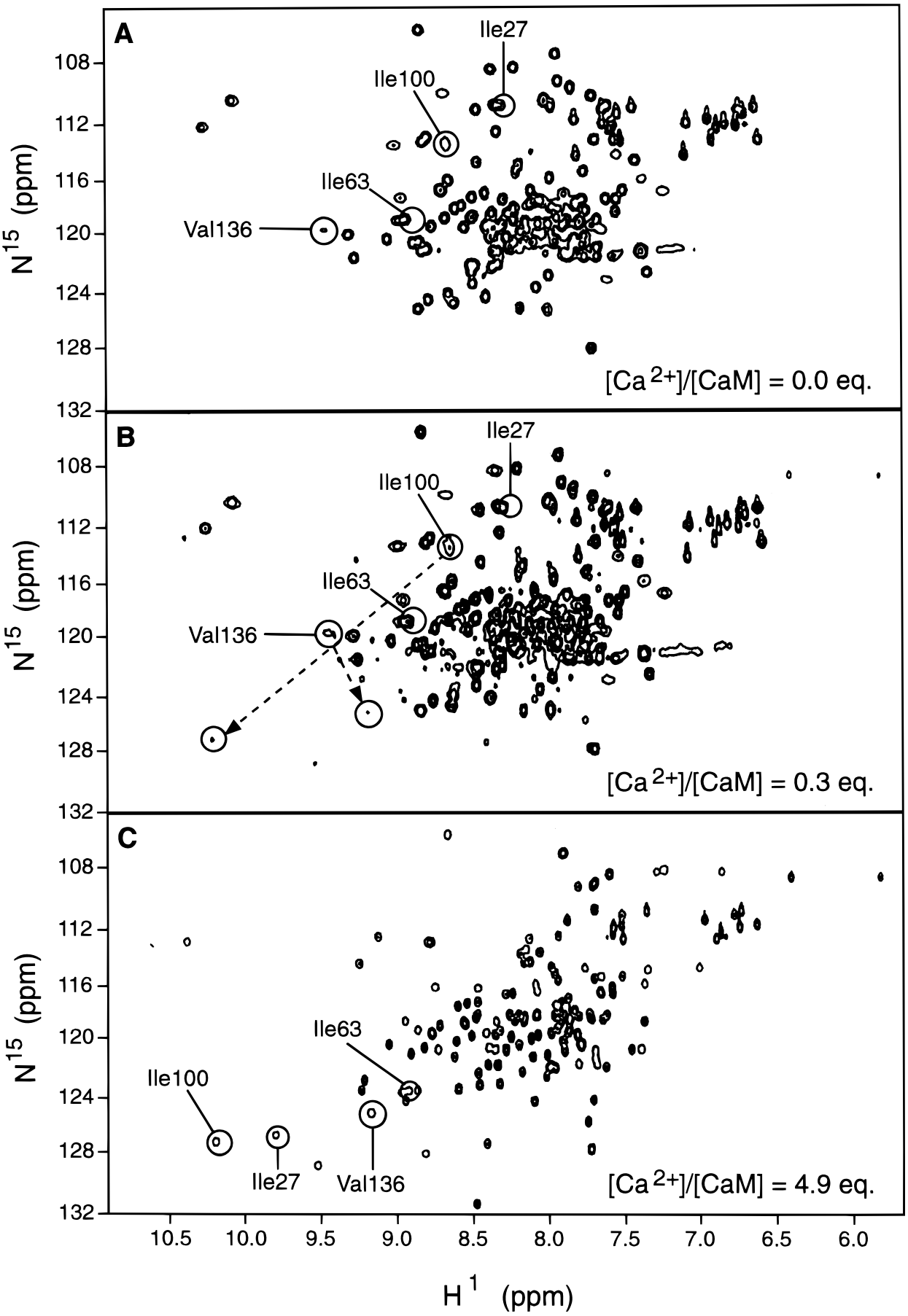

FIGURE 3: The ^{15}N-^{1}H HSQC spectrum for: (A) calmodulin at $[Ca^{2+}]/[CaM] = 0.0$ (apo-calmodulin), (B) calmodulin at $[Ca^{2+}]/[CaM] = 0.2725$ plotted at a very low contour level in order to show peaks corresponding to Ile100 (position 8, site III) and Val163 (position 8, site IV) in both the apo and holo forms, and (C) calmodulin at $[Ca_{2+}]/[CaM] = 4.9048$ (holo-calmodulin).

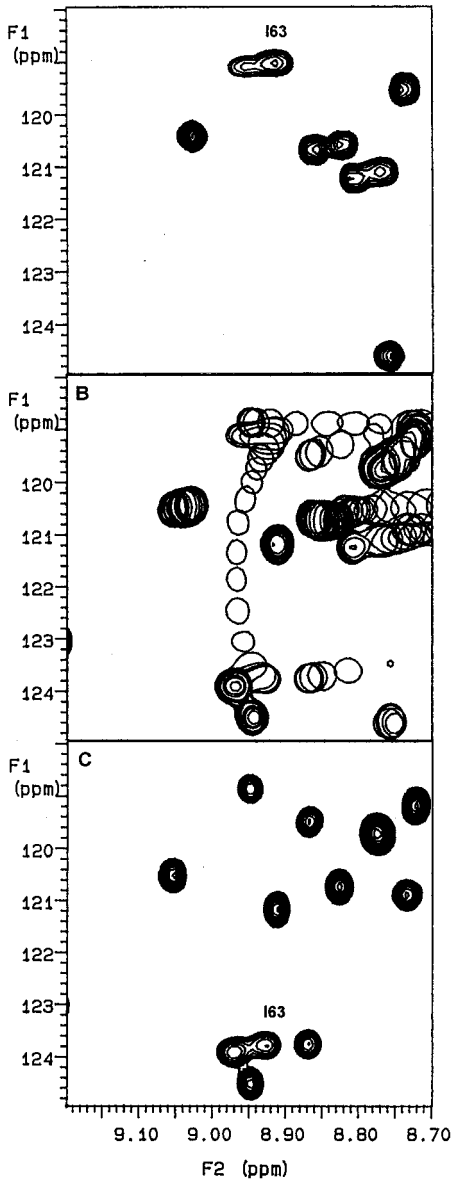

FIGURE 4: (A) Part of the ^{15}N-^{1}H HSQC spectrum for calmodulin at [Ca^{2+}]/[CaM] = 0.0 showing peak of Ile63 in apo-calmodulin. (B) Superposition of portions of ^{15}N-^{1}H HSQC spectra at different Ca^{2+} additions showing the progressive shift of the peak corresponding to Ile63 with increasing Ca^{2+} concentration. (C) Portion of ^{15}N-^{1}H HSQC spectrum for calmodulin at [Ca^{2+}]/[CaM] = 4.9048 showing peak of Ile-63 in holo-calmodulin.

of structural effects on amide linkages upon coordination of the carbonyl to metal ions. Cobalt complexes containing oxygen-bonded amide ligands have been shown to increase the polarization of the amide group and restrict the rotation about the carbon−nitrogen bond (*76*). A deshielding effect on the amide ^{15}N nucleus (+5 to +8 ppm) has been observed upon hydrogen bonding of the amide carbonyl oxygen (*75*) consistent with the stabilization of the polarized resonance form of the amide group (*77*). A similar deshielding effect of an amide nitrogen atom due to hydrogen bonding of the carbonyl has also been predicted from ab initio calculations by De Dios and co-workers (*78*). Consistently, a shielding effect for the amide carbonyl ^{17}O nucleus is observed upon hydrogen bonding of this carbonyl (*79* and references therein).

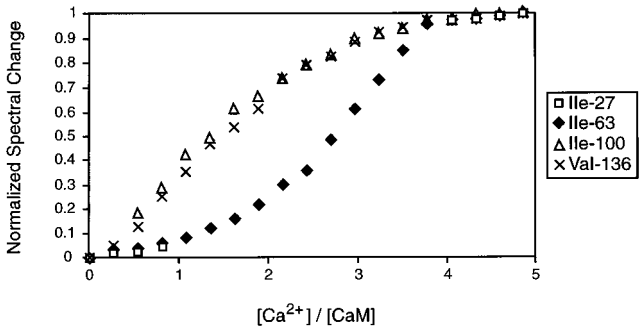

FIGURE 5: Ca^{2+} titration curves corresponding to residues Ile-27 (position 8, site I), Ile-63 (position 8, site II), Ile-100 (position 8, site III) and Val-163 (position 8, site IV) of calmodulin. Normalized spectral changes (chemical shifts for Ile27 and Ile63, and volumes for Ile100 and Val136) for the peaks corresponding to these residues are plotted as a function of the [Ca^{2+}]/[CaM] ratio.

(2) Changes in Side-Chain Conformation. The ^{15}N shielding in the NH groups of isoleucine or valine residues is sensitive to the side-chain conformation of these residues (*78*). According to reported ab initio calculations, the shielding for a NH in a valine fragment is predicted to be ~6 ppm more shielded when the H_α-C_α-C_β-H_β torsion angle is gauche(−) (−60°) rather than trans (180°) (*78*).

The change in π-polarization of the peptide bond upon metal coordination to the carbonyl oxygen is expected to yield a deshielding effect at the amide ^{15}N nucleus in all EF-hand loops. This effect is estimated to be +4 to +8 ppm, since no change of side-chain conformation for the residues in position 8 was observed for pseudo EF-hands, or for sites II or IV of canonical EF-hands.

The change in side-chain conformation upon metal coordination is expected to cause an additional deshielding effect of the amide ^{15}N nucleus for isoleucine or valine residues in site I or III consistent with a change in H_α-C_α-C_β-H_β torsion angle from gauche(−) in the apo state to trans in the calcium-bound form. Assuming that, as in the case of sites II or IV, the coordination of Ca^{2+} to the backbone carbonyl group has an effect on the ^{15}N amide nucleus in the range +4 to +8 ppm for sites I and III, the additional effect for residues in position 8 in site I or III due to the change in side-chain conformation can be estimated to be in the range +6 to +8 ppm. This is consistent with the theoretical prediction of +6 ppm by De Dios and co-workers (*78*).

The change in side-chain conformation explains the difference in ^{15}N chemical shift for ioleucine or valine residues in position 8 in the apo state. For sites I and III, the H_α-C_α-C_β-H_β torsion angle is ~−60° and the ^{15}N nuclei for these residues are more shielded (in the range 111−114 ppm) than they are in sites II and IV, where the H_α-C_α-C_β-H_β torsion angle is ~180° (^{15}N chemical shifts in the range 118−120 ppm).

In the calcium-bound state, the ^{15}N chemical shifts for these residues for all sites are in the range 124−127 ppm), consistent with the fact that the H_α-C_α-C_β-H_β torsion angle is ~180° in all cases (see Tables 5 and 6).

^{15}N Chemical Shifts as a Guide to Occupancy Of EF-Hand Metal-Binding Sites. The term *site specific* in this context is applied to the case in which a change in chemical shift in a site A residue is caused by binding of metal ion to site A regardless of the state of metal occupation of site B (for an EF-hand pair with two sites A and B).

For EF-hand pairs that can bind two metal ions (one ion to each site) the ^{15}N chemical shift difference of the residues in position 8 (or 10 for pseudo EF-hands) of each site upon metal binding provides a useful tool for determining unequivocally whether metal is bound to a particular EF-hand pair. For species where only one of the two sites is occupied, the binding of metal ion to this site is observed to cause a deshielding effect of +4 to +8 ppm to this amide ^{15}N nucleus. The ^{15}N chemical shift difference observed in position 8 (or 10 of pseudo EF-hands) upon metal binding in these species is therefore a useful means of obtaining site-occupation information in a direct and straightforward manner.

By contrast, the effect of the change in side-chain conformation on the amide ^{15}N nucleus upon metal binding occurs only in sites I or III and appears not to be site specific for the binding of Ca^{2+} to the same site, but rather depends on the binding of Ca^{2+} to the other site (site II or IV) when position 8 of site I or III is an isoleucine or valine in the gauche(−) conformation of the side chain in the apo form. Site I of N-cTnC does not bind Ca^{2+} but shows a ^{15}N chemical shift difference of +5.5 ppm for Ile36 (position 8, site I) on binding Ca^{2+} to site II only. In the apo state, Ile36 has a ^{15}N chemical shift of ca. 113.7 ppm consistent with a gauche(−) side-chain conformation for this residue. When Ca^{2+} is bound to site II and site I is calcium free, the ^{15}N chemical shift for Ile36 is ca. 119.2 ppm. This chemical shift is within the range expected for an isoleucine (or valine) in the position 8 of a canonical EF-hand loop with a trans side-chain conformation and with no Ca^{2+} ion bound to that site. This result is consistent with the observation that the binding of a calcium ion to site II in E31Q mutant of calmodulin shifts the ^1H resonance for the methyl group $C(\gamma)H_3$ of residue Ile 27 (position 8, site I) (*15*). The change in side-chain conformation for this situation is shown in Figure 2B.

In this context, it is of interest to examine the recently reported data for two mutant proteins, mutant E140Q of the C-terminal domain of calmodulin (*20*) and mutant E41A of the N-domain of skeletal troponin C (*39*).

E140Q:C−CaM. Mutant E140Q of the C-terminal domain of calmodulin (E140Q:C−CaM) lacks the bidentate carboxylate ligand in position 12 of calmodulin site IV and has a greatly reduced Ca^{2+} affinity in this site (*10*, *20*). Evenäs and co-workers estimate that at $[Ca^{2+}]/[E140Q:C-CaM] = 21$, the E140Q mutant domain is 97% in the $(Ca^{2+})_2$ form. However, the ^{15}N chemical shifts at position 8 show the following behavior.

(i) Residue Val136, position 8 of site IV, shifts from 119.3 ppm in the apo state to 120.0 ppm at $[Ca]_{total}/[E140Q:C-CaM]_{total} = 21$ (difference of +0.7 ppm). This ^{15}N chemical shift difference indicates no change in π-polarization of the N(8)−C(7)═O(7) peptide bond and it appears that in this mutant protein the carbonyl oxygen of residue 7 is not coordinated to Ca^{2+} in the normal way.

(ii) Residue Ile100, position 8 of site III, shifts from 113.2 ppm in the apo state to 121.7 ppm at $[Ca]_{total}/[E140Q:C-CaM]_{total} = 21$ (a difference of +8.5 ppm); this is as expected for the nonmutated site III binding Ca^{2+} and causing π-polarization of the N(8)−C(7)═O(7) peptide bond. For the same residue in the wild-type CaM, the ^{15}N chemical shift difference between apo and holo state is +13.4 ppm (Table 2); the conformation of the side chain for this residue in the apo state is gauche(−) consistent with the chemical shift of 113.2 ppm; it would seem that the H_α-C_α-C_β-H_β torsion angle of this residue has not changed to its trans conformation upon binding Ca^{2+} only to site III and not to site IV. This result is consistent with the observation that the change in side-chain conformation of the first site (site I or III) is dependent on the binding of Ca^{2+} to the alternate site IV. This is the only example encountered so far of an isoleucine (or valine) residue in position 8 of a canonical EF-hand that is in the gauche(−) side-chain conformation when that EF-hand site is binding Ca^{2+}; in Figure 2C, the change in side-chain conformation for this situation is shown.

E41A:N-sTnC. Mutant E41A of the N-domain of skeletal troponin C (N-sTnC), lacks the bidentate carboxylate ligand in position 12 of site I, resulting in a greatly reduced Ca^{2+} affinity for this site (*21*). Gagné and co-workers have reported that, at $[Ca]_{total}/[E41A:N-sTnC]_{total} = 6.119$, the E41A mutant is in the $(Ca^{2+})_2$ form (*39*). However, the analysis of the Ca^{2+}-induced ^{15}N chemical shift difference for the residues in position 8 of both sites (*21*) (Ile73 shifts from ca. 119.1 to ca. 127.9 ppm, ca. +8.2 ppm difference, Ile37 shifts from ca. 112.4 to ca. 118.2 ppm, ca. +5.8 ppm difference) indicate that they are fairly similar to those previously reported for N-domain of cardiac troponin C (Ile72 shifts from ca. 115.4 to ca. 127.2 ppm, ca. +11.8 ppm difference, Ile36 shifts from ca. 113.7 to ca. 119.2 ppm, ca. +5.5 ppm difference). The latter are known to be for the $(Ca^{2+})_1$ species (*40*), which suggests that the stoichiometries in these complexes of E41A:N-sTnC might require further investigation.

The examples discussed above highlight the potential use of these ^{15}N deshielding effects as a means for obtaining the metal-binding status of different binding sites in an EF-hand protein. The fact that only the change in π-polarization effect is site specific and not the change in side-chain conformation needs to be taken into account, especially in the analysis of half-saturated species.

^{15}N Chemical Shifts as Probes for Monitoring Metal-Binding Processes. For calmodulin, the calcium binding curves obtained from measurements of position 8 NH signals for a pair of sites within each domain were found to change in parallel (for sites I and II this statement is inferred from the few points on the curve obtained for site I). The binding curves corresponding to sites II and IV reflect the degree of occupation of each of these sites at different calcium concentrations (π-polarization effect only). For sites I and III, the corresponding curves reflect the degree of occupation of these sites (π-polarization effect) as well as the degree of occupation of the adjacent sites (change in the side-chain conformation effect, that depends on metal binding to site II or IV, respectively). If one of the sites in the C-domain were to be occupied before the other, then an intermediate peak would appear for site III. The fact that even from the first addition of Ca^{2+} peaks for I100 and V136 appear simultaneously (see Figure 3B) indicates that the species with both sites III and IV occupied is formed preferentially even in the presence of very little Ca^{2+} ion. This behavior is consistent with a significant positive intradomain cooperativity of calcium binding, thus the predominant species present during the titration are $[Ca_0N{\cdot}Ca_0C]CaM$, $[Ca_0N{\cdot}Ca_2C]CaM$, and $[Ca_2N{\cdot}Ca_2C]CaM$.

Concluding Remarks. The coordination of a backbone carbonyl to a metal ion localizes negative charge on the oxygen atom by enhancing the delocalization of the adjacent nitrogen lone pair. The π-polarization of this amide group shortens the C−N bond, conferring more rigidity to this portion of the polypeptide chain and leaving the NH proton more positive, capable of forming stronger hydrogen bonds (*80*). In an EF-hand pair, the disposition of the two backbone carbonyls that coordinate Ca^{2+} (one for each EF-hand loop) is such that the respective NHs are forming an antiparallel β-sheet. Upon Ca^{2+} coordination to both paired sites, the β-sheet hydrogen bonds are strengthened, bringing the two β-strands closer together. It is plausible that steric hindrance between the ethyl moiety of isoleucine 8 of the first site (I or III) and the H_β of isoleucine at position 8′ of the second site (II or IV) could cause the change in side-chain conformation that takes place in the first site upon binding of Ca^{2+} to the second site. The π-polarization of these peptide groups upon metal binding could play an important role in the molecular mechanism of cooperativity between paired metal-binding sites.

The ^{15}N properties discussed in the present work should prove useful for investigating Ca^{2+} binding to EF-hand sites within the calmodulin superfamily. Despite their common secondary structural motifs, the Ca^{2+}-binding affinities of EF-hand pairs vary over at least 3 orders of magnitude (*81*). Although several groups have proposed structure−function relationships (*25*, *82*−*84*), the mechanisms through which structural variations modulate binding affinity remain incompletely defined. The correlation of ^{15}N chemical shifts with structure presented in this work should also prove useful for investigating binding of metals other than Ca^{2+} to EF-hand sites (*85*, *86*), for characterizing metal binding to new EF-hand proteins (*87*) or EF-hand chimera proteins (*14*) or EF-hand peptide analogues (*88*, *89*), and for analyzing the binding capacity of novel variant EF-hand loops (*90*−*92*) and of EF-hand sites containing mutated residues (*20*, *21*, *93*, *94*).

ACKNOWLEDGMENT

We are grateful to Annalisa Pastore (NIMR, Mill Hill) for providing umpublished ^{15}N chemical shift assignments for apo-spectrin and for comments on the manuscript, to Mitsuhiko Ikura (University of Toronto) for providing unpublished ^{15}N chemical shift assignments for apo-calmodulin, to Kathy Beckingham (Rice University, Houston, TX) for supplying the pOTSNco12 vector containing the cDNA coding for *Drosophila melanogaster* calmodulin, to John E. McCormick for expert technical assistance, and to Tom A. Frenkiel for assistance with the NMR experiments.

REFERENCES

1. Finn, B. E., Evenäs, J., Drakenberg, T., Waltho, J. P., Thulin, E., and Forsén, S. (1995) *Nat. Struct. Biol. 2*, 777−783.
2. Kuboniwa, H., Tjandra, N., Grzesiek, S., Ren, H., Klee, C. B., and Bax, A. (1995) *Nat. Struct. Biol. 2*, 768−776.
3. Travé, G., Lacombe P−J., Pfuhl, M., Saraste, M., and Pastore, A. (1995) *EMBO J. 14*, 4922−4931.
4. Zhang, M., Tanaka, T., and Ikura, M. (1995) *Nat. Struct. Biol. 2*, 758−767.
5. Kretsinger, R. H., and Nockolds, C. E. (1973) *J. Biol. Chem. 248*, 3313−3326.
6. Sellers, P., Laynez, J., Thulin, E., and Forsén, S. (1991) *Biophys. Chem. 39*, 199−204.
7. Luanrilliet, Y., Milos, M., and Cox, J. A. (1992) *Eur. J. Biochem. 208*, 133−138.
8. Kilhoffer, M. C., Kubina, M., Travers, F., and Haiech, J. (1992) *Biochemistry 31*, 8098−8106.
9. Török, K., Lane, A. N., Martin, S. R., Janot, J.-M., and Bayley, P. M. (1992) *Biochemistry 31*, 3452−3462.
10. Maune, J. F., Beckingham, K., Martin, S. R., and Bayley, P. M. (1992) *Biochemistry 31*, 7779−7786.
11. Gagné, S. M., Tsuda, S., Li, M. X., Chandra, M., Smillie, L. B., and Sykes B. D. (1994) *Protein Sci. 3*, 1961−1974.
12. Martin, S. R., Bayley P. M., Brown S. E., Porumb T., Zhang M., and Ikura M. (1996) *Biochemistry 35*, 3508−3517.
13. Mukherjea, P., Maune, J. F, and Beckingham, K. (1996) *Protein Sci. 5*, 468−477.
14. George, S. E., Su, Z., Fan, D., Wand, S., and Johnson, J. D. (1996) *Biochemistry 35*, 8307−8313.
15. Starovasnik, M. A., Su, D.-R., Beckingham, K., and Klevit R. E. (1992) *Protein Sci. 1*, 245−253.
16. Moser, M. J., Lee, S. Y., Klevit, R. E., and Davis, T. N. (1995) *J. Biol. Chem. 270*, 20643−20652.
17. Pedigo, S., and Shea, M. A. (1995) *Biochemistry 34*, 10676−10689.
18. Li, M. S., Gagné, S. M., Tsuda, S., Kay, C. M., Smillie, L. B., and Sykes, B. D. (1995) *Biochemistry 34*, 8330−8340.
19. Ohki, S., Miura, K., Saito, M., Nakashima, K., Maekawa, H., Yazawa, M., Tsuda, S., and Hikichi, K. (1996) *J. Biochem. 119*, 1045−1055.
20. Evenäs, J., Thulin, E., Malmendal A., Forsén, S., and Carlström, G. (1997) *Biochemistry 36*, 3448−3457.
21. Li, M. X., Gagné, S. M., Spyracopoulos, L., Kloks, C. P. A. M., Audette, G., Chandra, M., Solaro, R. J., Smillie, L. B., and Sykes, B. D. (1997) *Biochemistry 36*, 12519−12525.
22. McPhalen, C. A., Strynadka, N. C. J., and James, M. N. G. (1991) *Adv. Protein Chem. 42*, 77−144.
23. Strynadka, N. C. J., and James, M. N. G. (1989) *Annu. Rev. Biochem. 58*, 951−998.
24. Falke, J. J., Drake, S. K., Hazard, A. L., and Peersen, O. B. (1994) *Q. Rev. Biophys. 27*, 219−290.
25. Linse, S., and Forsén, S. (1995) in *Adv. Second Messenger Phosphoprotein Res. 30* (Means, A. R., Ed.) pp 89−151, Raven Press Ltd., New York.
26. Ikura, M., Kay, L. E., and Bax, A. (1990) *Biochemistry 29*, 4659−4667.
27. Ikura, M., Kay, L. E., Krinks, M., and Bax, A. (1990) *Biochemistry 30*, 5498−5504.
28. Ikura, M., Clore, G. M., Gronenborn, A. M., Zhu, G., Klee, C. B., and Bax, A. (1992) *Science 256*, 632−638.
29. Skelton, N. J., Akke, M., Kördel, J., Thulin, E., Forsén, S., and Chazin, W. J. (1992) *FEBS Lett. 303*, 136−140.
30. Akke, M., Forsén, S., and Chazin, W. J. (1993) *Magn. Reson. Chem. 31*, S128−S132.
31. Ames, J. B., Tanaka, T., Stryer, L., and Ikura, M. (1994) *Biochemistry 33*, 10743−10753.
32. Findlay, W. A., Soennichsen, F. D., and Sykes, B. D. (1994) *J. Biol. Chem. 269*, 6773.
33. Padilla, A., Cavé, A., Parello, J., Etienne, G. and Baldellon, C. (1994) NMR structures of parvalbumin (alpha lineage, PI 5.0) complexed with Ca^{2+} (2PAS) taken from the PDB (ref *95*).
34. Slupsky, C. M., and Sykes B. D. (1995) *Biochemistry 34*, 15953−15964.
35. Slupsky, C. M., Reinach, F. C., Smillie, L. C. and Sykes, B. D. (1995) *Protein Sci. 4*, 1279−1290.
36. Urbauer, J. L., Short, J. H., Dow, L. K., and Wand, A. J. (1995) *Biochemistry 34*, 8099−8109.
37. Henzl, M. T., Likos, J. J., and Hutton, W. C. (1996) *Protein Pept. Lett. 31*, 59−66.
38. Kilby, P. M., Van Eldik, L. J., and Roberts, G. C. K. (1996) *Structure 4*, 1041−1052.
39. Gagné, S. M., Li, M. X., and Sykes, B. D. (1997) *Biochemistry 36*, 4386−4392.

40. Spyracopoulos, L., Li, M. X., Sia, S. K., Gagné, S. M., Kloks, C. P. A. M., Chandra, M., Solaro, R. J., and Sykes, B. D. (1997) *Biochemistry 36*, 12138−12146.
41. Amburgey, J. C., Abildgaard, F., Starich, M. R., Shah, S., Hilt, D. C., and Weber, D. J. (1995) *J. Biomol. NMR 6*, 171−179.
42. Smith, S. P., and Shaw, G. S. (1997) *J. Biomol. NMR* 10, 77−88.
43. Maune, J. F., Klee, C. B., and Beckingham, K. (1992) *J. Biol. Chem. 267*, 5286−5295.
44. Shatzman, A. R., and Rosenberg, M. (1987) *Methods Enzymol. 152*, 661−673.
45. Browne, J. P., Strom, M., Martin, S. R., and Bayley, P. M. (1997) *Biochemistry 36*, 9550−9561.
46. Bodenhausen, G., and Ruben, D. J. (1980) *Chem. Phys. Lett. 69*, 185.
47. Mori, S., Abeygunawardana, C., O'Neil Johnson, M., and van Zijl, P. C. M. (1995) *J. Magn. Reson. B 108*, 94−98.
48. Sklenar, V., Piotto, M., Leppik, R., and Saudek, V. (1993) *J. Magn. Reson. A 102*, 241−245.
49. Bartels, C., Xia, T., Billeter, M., Güntert, P., and Wüthrich, K. (1995) *J. Biomol. NMR 5*, 1−10.
50. Wishart, D. S., Bigam, C. G., Yao J., Abildgaard F., Dyson, H. J., Oldfield, E., Markley, J. L., and Sykes, B. D. (1995) *J. Biomol. NMR 6*, 135−140.
51. Strynadka, N. C. J., and James, M. N. G. (1991) *Curr. Opin. Struct. Biol. 1*, 905−914.
52. Crivici, A., and Ikura, M. (1995) *Annu. Rev. Biophys. Biomol. Struct. 24*, 85−116.
53. Schäfer, B. W., and Heizmann, C. W. (1996) *Trends Biochem. Sci. 21*, 134−140.
54. Heizmann, C. W., and Hunziker, W. (1991) *Trends Biochem. Sci 16*, 98−103.
55. Chakrabarti, P. (1990) *Biochemistry 29*, 651−658.
56. Akke, M., Forsén, S., and Chazin, W. J. (1991) *J. Mol. Biol. 220*, 173−189.
57. Kördel, J., Pearlman, D. A., and Chazin, W. J. (1997) *J. Biomol. NMR 10*, 231−243.
58. Swain, A. L., Kretsinger, R. H., and Amma, E. L. (1989) *J. Biol. Chem. 264*, 16620−16628.
59. Kumar, V. D., Lee, L., and Edwards, B. F. P. (1990) *Biochemistry 29*, 1404−1412.
60. Declercq, J. P., Tinant, B., Parello, J., and Rambaud, J. (1991) *J. Mol. Biol. 220*, 1017−1039.
61. Svensson, L. A., Thulin, E., and Forsén, S. (1992) *J. Mol. Biol. 223*, 601−606.
62. Roquet, F., Declercq, J. P., Tinant, B., Rambaud, J., and Parello, J. (1992) *J. Mol. Biol. 223*, 705−720.
63. Akke, M., Drakenberg, T., and Chazin, W. J. (1992) *Biochemistry 31*, 1011−1020.
64. Akke, M., Forsén, S., and Chazin. W. J. (1995) *J. Mol. Biol. 252*, 102−121.
65. Satyshur, K. A., Pyzalska, D., Greaser, M., Rao, S. T., and Sundaralingam, M. (1994) *Acta Crystallogr. Sect. D 50*, 40−49.
66. Ban, C., Ramakrishnan, B., Ling, K. Y., Kung, C., and Sundaralingam, M. (1994) *Acta Crystallogr. Sect. D 50*, 50−63.
67. Skelton, N. J., Kordel, J., and Chazin, W. J. (1995) *J. Mol. Biol. 249*, 441−462.
68. Rao, S. T., Satyshur, K. A., Greaser, M. L., and Sundaralingam, M. (1996) *Acta Crystallogr. Sect. D 52*, 916−922.
69. Reuben, J., and Fiat, D. (1969) *J. Chem. Phys. 51*, 4918−4927.
70. Linse, S., Helmersson, A., and Forsén, S. (1991) *J. Biol. Chem. 266*, 8050−8054.
71. Porumb, T. (1994) *Anal. Biochem. 220*, 227−237.
72. Bayley, P. M., Findlay, W. A., and Martin, S. R. (1996) *Protein Sci. 5*, 1215−1228.
73. Milos, M, Schaer, J.-J., Comte, M., and Cox, J. A. (1986) *Biochemistry 25*, 6279−6287.
74. Levy, G. C., and Lichter, R. L. (1979) *Nitrogen-15 NMR spectroscopy*, Wiley-Interscience, New York.
75. Witanowski, M., Stefaniak, L., and Webb, G. A. (1993) *Annu. Rep. NMR Spectrosc. 25*, 2−469.
76. Angus, P. M., Fairlie, D. P., and Jackson W. G. (1993) *Inorg. Chem. 32*, 450−459.
77. Gattegno, D., Hawkes, G. E., and Randall, E. W. (1976) *J. Chem. Soc., Perkin Trans. II*, 1527−1531.
78. De Dios, A. C., Pearson, J. G., and Oldfield, E. (1993) *Science 260*, 1491−1496.
79. Contreras, R. H., Biekofsky, R. R., Esteban, A. L., Diez, E., and San Fabian, J. (1996) *Magn. Reson. Chem. 34*, 447−452.
80. Jeffrey, G. A., and Saenger, W. (1991) *Hydrogen bonding in biological structures*, Springer-Verlag, Berlin Heidelberg.
81. Kretsinger, R. H. (1980) *CRC Crit. Rev. Biochem. 5*, 119−173.
82. Reid, R. E., and Hodges, R. S. (1980) *J. Theor. Biol. 84*, 401−444.
83. Da Silva, A. C. R., De Araujo, A. H. B., Herzberg, O., Moult, J., Sorenson, M., and Reinach, F. C. (1993) *Eur. J. Biochem. 213*, 599−604.
84. Linse, S., and Chazin, W. J. (1995) *Protein Sci. 4*, 1038−1044.
85. Snyder, E. E., Buoscio, B. W., and Falke, J. J. (1990) *Biochemistry 29*, 3937−3943.
86. Ohki, S., Ikura, M., and Zhang, M. (1997) *Biochemistry 36*, 4309−4316.
87. Gopal, B., Swaminathan, C. P., Bhattacharya, S., Bhattacharya, A., Murthy, M. R. N., and Surolia, A. (1997) *Biochemistry 36*, 10910−10916.
88. Marsden, B. J., Hodges, R. S., and Sykes, B. D. (1989) *Biochemistry 28*, 8839−8847.
89. Sharma, Y., Chandani S., Sukhaswami, M. B., Uma, L., Balasubramanian, D., and Fairwell T. (1997) *Eur. J. Biochem. 243*, 42−48.
90. Rayment, I., Rypniewski, W. R, Schmidt-Base, K., Smith, R., Tomchick, R. D., Benning, M. M., Winklemann, D. A., Wesenberg, G., and Holden, H. M. (1993) *Science 261*, 50−58.
91. Hohenester, E., Maurer, P., Hohenadl, C., Timpl, R., Jansonius, J. N., and Engel, J. (1996) *Nat. Struct. Biol. 3*, 67−73.
92. Blanchard, H., Grochulski, P., Li, Y., Arthur, S. C., Davies, P. L., Elce, J. S., and Cygler, M. (1997) *Nat. Struct. Biol. 4*, 532−538.
93. Wimberley, B., Thulin, E., and Chazin, W. J. (1995) *Protein Sci. 4*, 1045−1055.
94. Wu, X., and Reid, R. E. (1997) *Biochemistry 36*, 3608−3616.
95. Bernstein, F. C., Koetzle, T. F., Williams, G. J. B, Meyer, E. F., Jr., Brice, M. D., Rodgers, J. R., Kennard, O., Shimanouchi, T., and Tasumi, M. (1977) *J. Mol. Biol. 112*, 535−542.

BI9800449